

The Impact of Partial Occlusion on Pedestrian Detectability

Shane Gilroy^{1,2}, Darragh Mullins¹, Edward Jones¹, Ashkan Parsi¹ and Martin Glavin¹

¹National University of Ireland, Galway, Ireland

²Atlantic Technological University, Ireland

Abstract

Robust detection of vulnerable road users is a safety critical requirement for the deployment of autonomous vehicles in heterogeneous traffic. One of the most complex outstanding challenges is that of partial occlusion where a target object is only partially available to the sensor due to obstruction by another foreground object. A number of leading pedestrian detection benchmarks provide annotation for partial occlusion, however each benchmark varies greatly in their definition of the occurrence and severity of occlusion. Recent research demonstrates that a high degree of subjectivity is used to classify occlusion level in these cases and occlusion is typically categorized into 2-3 broad categories such as “partially” and “heavily” occluded. This can lead to inaccurate or inconsistent reporting of pedestrian detection model performance depending on which benchmark is used. This research introduces a novel, objective benchmark for partially occluded pedestrian detection to facilitate the objective characterization of pedestrian detection models. Characterization is carried out on seven popular pedestrian detection models for a range of occlusion levels from 0-99%. Results demonstrate that pedestrian detection performance degrades, and the number of false negative detections increase as pedestrian occlusion level increases. Of the seven popular pedestrian detection routines characterized, CenterNet has the greatest overall performance, followed by SSDlite. RetinaNet has the lowest overall detection performance across the range of occlusion levels.

1. Introduction

Accurate and robust pedestrian detection systems are an essential requirement for the safe navigation of autonomous vehicles in heterogeneous traffic. The SAE J3016 standard [1] defines levels of driving automation ranging from Level 0, where the vehicle contains zero automation and the human driver is in complete control, to level 5 where the vehicle is solely responsible for all perception and driving tasks in all scenarios. The progression from automa-

tion levels 3-5 requires a significant increase in assumption of responsibility by the vehicle, placing progressively increasing demands on the performance of pedestrian detection systems to inform efficient path planning and to ensure the safety of vulnerable road users. Despite recent improvements in pedestrian detection systems, many challenges still exist before we reach the object detection capabilities required for safe autonomous driving. One of the most complex and persistent challenges is that of partial occlusion, where a target object is only partially available to the sensor due to obstruction by another foreground object. The frequency and variety of occlusion types in the automotive environment is large and diverse as pedestrians navigate between vehicles, buildings, traffic infrastructure, other road users. Pedestrians can be occluded by static or dynamic objects, may inter-occlude (occlude one another) such as in crowds, and self-occlude - where parts of a pedestrian overlap. Leading pedestrian detection systems claim a detection performance of approximately 65%-75% of partially and heavily occluded pedestrians respectively using current benchmarks [2] [3] [4] [5]. However, recent research [6] demonstrates that the definition of the occurrence and severity of occlusion varies greatly, and a high degree of subjectivity is used to categorize pedestrian occlusion level in each benchmark. In addition, occlusion is typically split into 2-3 broad, loosely defined, categories such as “partially” or “heavily” occluded [7] [8] [9]. A knowledge gap exists for objective, detailed occlusion level analysis for pedestrian detection across the complete spectrum of occlusion levels. Use of an objective, fine grained occlusion specific benchmark will result in more objective, consistent and detailed analysis of pedestrian detection algorithms for partially occluded pedestrians.

This research uses a novel, objective benchmark for partially occluded pedestrian detection to facilitate the objective characterization of pedestrian detection models. Objective characterization of occluded pedestrian detection performance is carried out for seven popular pedestrian detection routines for a range of occlusion levels from 0-99%. The contributions of this research are: 1. A novel, objective, test benchmark for partially occluded pedestrian de-

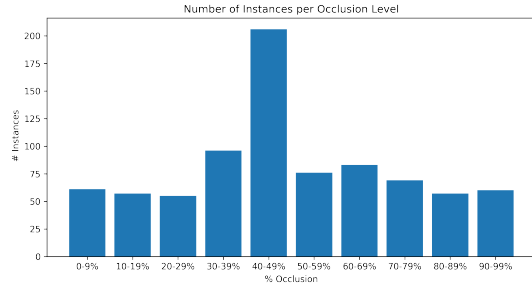


Figure 1. Dataset Statistics. The number of pedestrian instances per occlusion level. The custom dataset contains 820 pedestrian instances under progressive levels of occlusion from 0-99%.

tection is presented. 2. Objective characterization of pedestrian detection performance is carried out for seven popular pedestrian detection routines.

2. Related Work

A number of popular pedestrian detection benchmarks provide annotation of pedestrian occlusion level to determine the relative detection performance for partially occluded pedestrians. Dollar *et al* [20] provides analysis on occluded pedestrians based on the Caltech Pedestrian Dataset [21]. Caltech Pedestrian estimates the occlusion ratio of pedestrians by annotating 2 bounding boxes, one for the visible pedestrian area and one for the annotators estimate of the total pedestrian area. Pedestrians are categorised into 2 occlusion categories, “partially occluded”, defined as 1-35% occluded and “heavily occluded”, defined as 35-80% occluded. Any pedestrians suspected to be more than 80% occluded are labelled as fully occluded. Analysis of the frequency of occlusion on the Caltech Pedestrian Dataset demonstrated that over 70% of pedestrians were occluded in at least one frame, highlighting the frequency of occurrence of pedestrian occlusion in the automotive environment. The Eurocity Persons [9] Dataset categorizes pedestrians according to three occlusion levels: low occlusion (10%-40%), moderate occlusion (40%-80%), and strong occlusion (larger than 80%). Classification is carried out by human annotators in a similar manner to the Caltech Pedestrian Dataset. The full extent of the occluded pedestrian is estimated, and the approximate level of occlusion is then estimated to be within one of the three defined categories. Citypersons [8] calculate occlusion levels by drawing a line from the top of the head to the middle of the two feet of the occluded pedestrian. Human annotators are required to estimate the location of the head and feet if these are not visible. A bounding box is then generated for the estimated full pedestrian area using a fixed aspect ratio of 0.41(width/height). This is then compared to the visible

area bounding box to denote occlusion level. These estimates of occlusion level are then categorized into two levels, “reasonable” ($\leq 35\%$ occluded) and “heavy occlusion” (35%-75%). Similar approaches are taken in [22] [23] [24] [25] [26]. The Kitti Vision Benchmark [7] and Multispectral Pedestrian Dataset [27] tasked human annotators with marking each pedestrian bounding box as “visible”, “semi-occluded”, “fully-occluded”. Although these methods are useful for the relative comparison of detection performance on specific datasets, the occlusion categories used are broad (usually 2 to 3 categories), are inconsistent from benchmark to benchmark, and involve a high degree of subjectivity by the human annotator [6]. A knowledge gap exists for a detailed, objective benchmark to compare pedestrian detection performance for partially occluded pedestrians. Many pedestrian detection analysis papers [20] [22] [28] [29] [30] [31] [32] [33] [34] [35] and occlusion-specific survey papers [2] [3] [5] [36] [37] highlight the outstanding challenges posed by occluded pedestrians, however, no known objective characterization of pedestrian detection performance spanning the spectrum of occlusion levels has been carried out to date.

Gilroy *et al* [38] describes an objective method of occlusion level annotation and visible body surface area estimation of partially occluded pedestrians. Keypoint detection is applied to identify semantic body parts and findings are cross-referenced with a visibility score and the pedestrian mask in order to confirm the presence or occlusion of each semantic part. A novel method of 2D body surface area estimation based on the “Wallace rule of Nines” [6] [39] is then used to quantify the total occlusion level of pedestrians.

3. Methodology

A novel occluded pedestrian test dataset, containing 820 person instances in 724 images, has been created in order to characterize pedestrian detection performance across a range of occlusion levels from 0 to 99% occluded. A diverse mix of images are used ensure that a wide variety of target pedestrians, pedestrian poses, backgrounds, and occluding objects are represented. The dataset is sourced from three main categories of images: 1) The “occluded body” subset of the partial re-identification dataset “Partial ReID” provided by Zheng *et al* [40], 2) The Partial ReID “whole body” subset [40] with custom superimposed occlusions and 3) Images collated from publicly available sources including [6] [8] [9] [41]. All images are annotated using the objective occlusion level classification method described in [38]. Complex cases at very high occlusion rates were manually verified using the method of 2D body surface area estimation presented in [6]. Each occlusion level contains a minimum of 55 pedestrian instances. Dataset statistics by occlusion level and a sample of the test dataset can be seen in Figure 1 and Figure 2 respectively.

Table 1. Overview of Pedestrian Detection Models.

Model	Classifier	Training Data	Weights Source	Performance (mAP)
FasterRCNN [10]	ResNet-50 FPN	COCO	Voxel51 [11]	0.398
MaskRCNN [12]	ResNet-50 FPN	COCO	Voxel51 [11]	0.411
R-FCN [13]	ResNet-101	COCO	Voxel51 [11]	0.411
SSD [14]	VGG16	COCO	Torchvision [15]	0.412
SSDlite [16] [17]	MobileNetV3 Large	COCO	Torchvision [15]	0.464
RetinaNet [18]	ResNet-50 FPN	COCO	Voxel51 [11]	0.361
CenterNet [19]	Hourglass-104	COCO	Voxel51 [11]	0.533

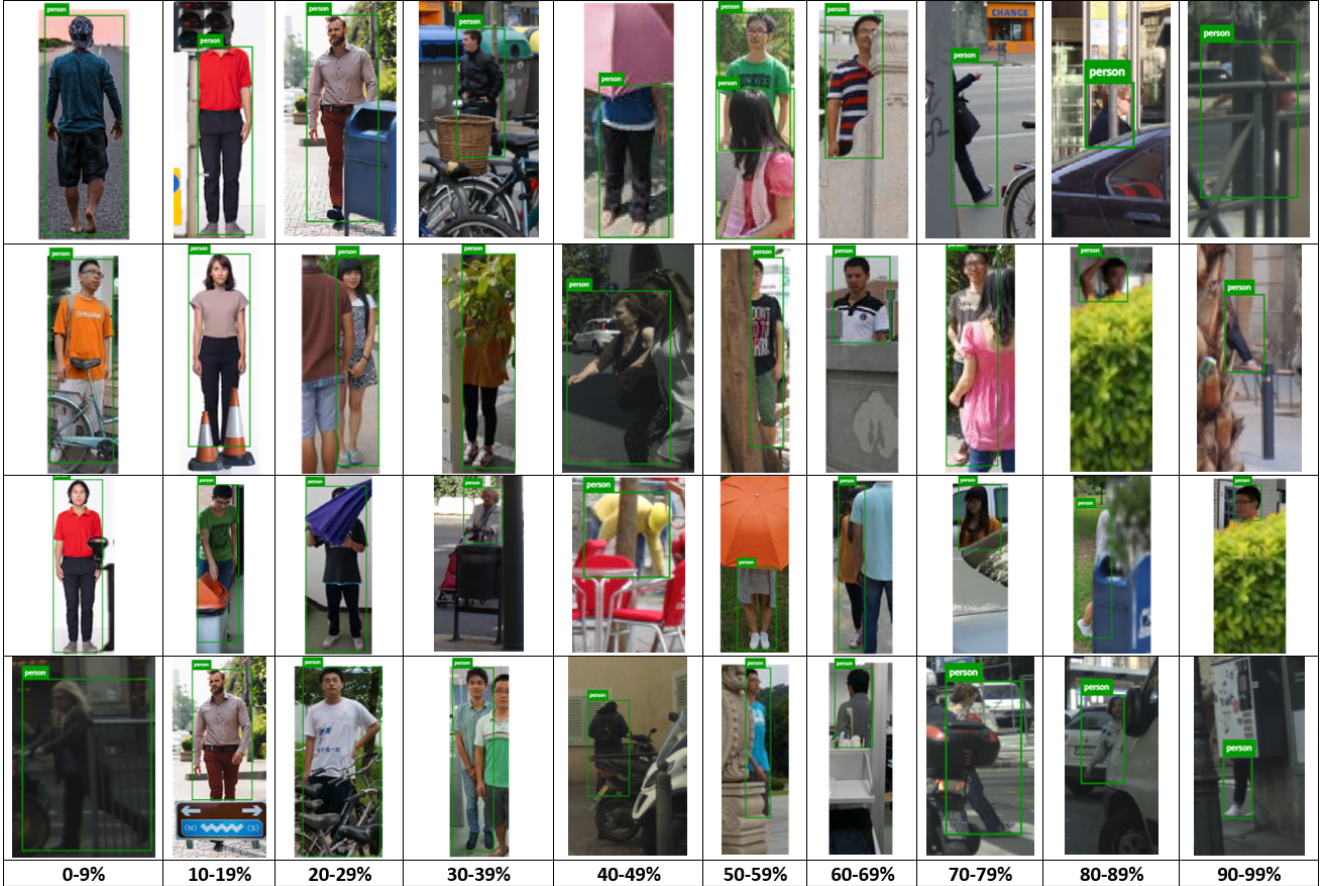


Figure 2. Dataset Sample. An example of dataset images for each level of occlusion. The custom dataset contains 820 pedestrian instances containing a wide range of pedestrian poses and occluding objects. All images are compiled from publicly available sources.

3.1. Pedestrian Detection Models

Performance characterization was carried out on seven popular pedestrian detection models. All models use publicly available pretrained weights from two popular model zoos [15] [11] and are trained using the COCO “train 2017” dataset [42]. An overview of the pedestrian detection models can be seen in Table 1. The pedestrian detection mod-

els chosen for characterization can be divided into 3 categories: Two-Stage Frameworks, One-Stage Frameworks and Keypoint Estimation. Two-stage frameworks such as FasterRCNN [10], MaskRCNN [12] and R-FCN [13] apply two separate networks to perform classification. One network is used to propose regions of interest and a dedicated second network performs object detection [43]. One-

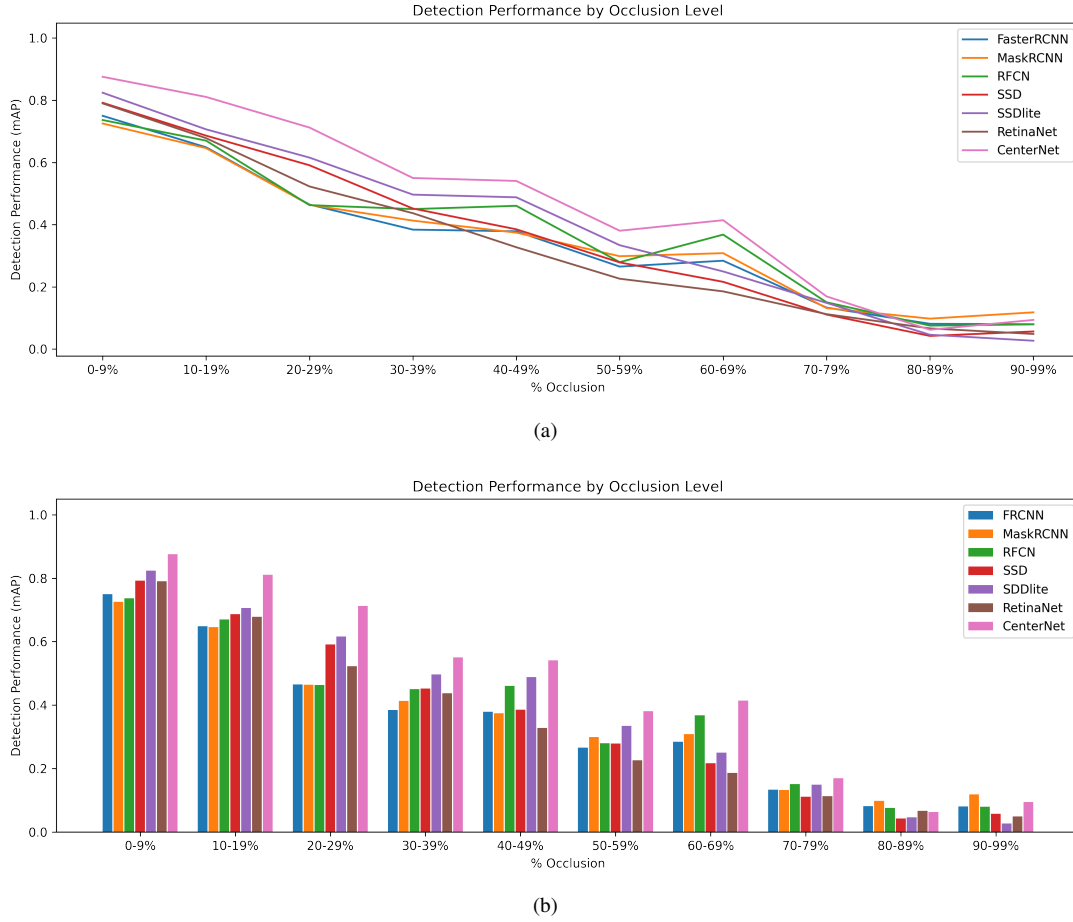


Figure 3. Detection Performance by Occlusion Level. Pedestrian detection performance of seven popular pedestrian detection models is displayed for images containing progressive levels of occlusion. Pedestrian detection performance declines in a linear manner as the level of pedestrian occlusion is increased, (a). CenterNet [19] is the highest performing detection model for pedestrians up to 80% occluded, (b).

stage frameworks such as RetinaNet [18], SSD [14] and SSDLite [16] [17] attempt to reduce computation and increase speed by performing object detection using a single feed forward convolutional network that does not interact with a region proposal module. RetinaNet also implements a novel method of “focal loss” which is used to reduce the imbalance between foreground and background classes during training with a view to increasing detection precision. CenterNet [19] takes an alternative approach based on key-point estimation. Objects are represented as a single point at their bounding box center identified by a heat map generated using a fully convolutional network. Other object features such as object size, orientation and pose are then regressed directly from the image features at the center location.

3.2. Experiments

Detection performance is analyzed for the complete test dataset, and for each occlusion range from 0-9% to 90-99%, for pedestrian detection models to assess the impact of progressive levels of occlusion on the detectability of pedestrians. Experiments are carried out with an intersection over union (IoU) of 0.5. Analysis is carried out using Voxel51 [44] and COCO style evaluation metrics. A summary of the results are shown in Figure 3, Figure 4 and Figure 5.

4. Results and Analysis

Results demonstrate that pedestrian detection performance (mAP) declines as the level of pedestrian occlusion increases, Figure 3(a). The number of false negative detections increase as occlusion level increases, Figure 5(e) and in general, the number of true positive detections begin to significantly decrease as occlusion level increases

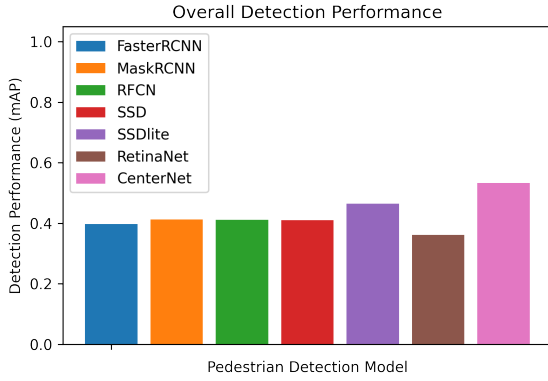


Figure 4. Overall Detection Performance. CenterNet has the greatest overall performance with a mAP of 0.533, followed by SSDlite (mAP = 0.464). RetinaNet has the lowest overall performance on the test dataset with a mAP of 0.361.

for pedestrians more than 50% occluded, Figure 5(a). As shown in Figure 4, of the seven popular pedestrian detection models analyzed, CenterNet [19] has the greatest overall detection performance for partially occluded pedestrians with an overall mAP of 0.533, followed by SSDlite [16] [17] with a total dataset mAP of 0.464. MaskRCNN [12] has the greatest detection performance for pedestrians occluded more than 80%, Figure 4(b). RetinaNet [18] is the lowest performing overall on the test data with a mAP of 0.361. RetinaNet’s true positive detections begin to degrade in a linear fashion once pedestrians are more than 30% occluded and this model has the highest number of false negatives for pedestrians more than 30% occluded, Figure 5(a) and 5(e). Single Shot Detectors, SSD [14] and SSDlite [16] [17] have the highest number of true positive detections at high levels of occlusion, Figure 5(a), and maintain a very high level of true positive detections up to 60% occlusion, however their false positive rate is in the region of 100 times larger than popular two stage detectors such as FasterRCNN [10] and RFCN [13], Figure 5(b), and approximately 16 times larger than MaskRCNN [12], Figure 5(c). Unlike false negatives, the number of false positives per image does not appear to be significantly impacted by the occlusion level as these are not typically related to the target pedestrian in an image. SSDlite [16] [17] outperforms SSD [14] for almost all levels of occlusion despite having a higher number of false positive detections. MaskRCNN [12] has a higher percentage of true positives than Faster RCNN [10] for pedestrians over 40% occluded, however, it has around 4 times more false positive detections for the same data, Figure 5. Mask RCNN, RFCN and SSD all have similar overall performance on the test dataset, however, MaskRCNN and RFCN have a higher detection performance than SSD for

pedestrians that are more than 60% occluded, Figure 3(b).

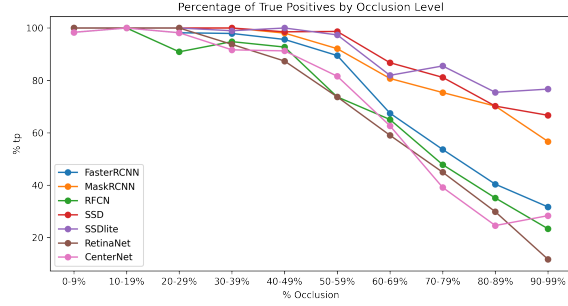
Figure 6 compares the output from a two stage detector, FasterRCNN, with a one stage detector, SSD, for an occluded pedestrian. Two stage detectors first generate key regions of interest before applying object detection, one stage detectors directly apply object detection to the entire image. Figure 6 demonstrates that for the same image, FasterRCNN produces 4 detection outputs (1 true positive with 88% confidence and 3 false positives), Figures 6(b) and 6(c), whereas SSD produces 84 detection outputs (1 true positive with 20% confidence and 83 false positives), Figures 6(d) and 6(e). This indicates that all detection models must not be treated equally in the design of a pedestrian detection system. The characteristics of the detection model used must be taken into account further downstream in the object detection system, as some model outputs may be less reliable than others for safety critical systems.

4.1. Key Semantic Parts

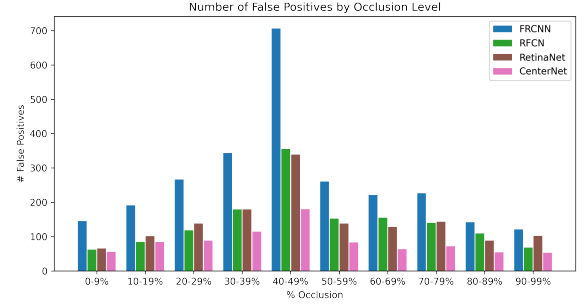
Further analysis has been carried out to determine the impact that the visibility of a pedestrian’s head has on the detection of occluded pedestrians. The dataset was split into two subsets: 1) Only images where the target pedestrian’s head is visible and 2) Only images where the target pedestrian’s head is occluded. Of the 820 pedestrian instances, the target pedestrian’s head is visible in 582 instances and is occluded in 252 instances. Figure 7(a) displays the percentage of pedestrian instances with their head visible across each of the occlusion levels. Three pedestrian detection models, FasterRCNN, RetinaNet and SSD were then tested on both data subsets across the occlusion range. This experiment demonstrates that, regardless of whether a pedestrian’s head is visible, a distinct declining profile in detection performance is observed as pedestrian occlusion level increases, Figures 7(b), 7(c) and 7(d). This indicates that the detection models under test are not overly reliant on head visibility for the classification of partially occluded pedestrians.

5. Conclusion

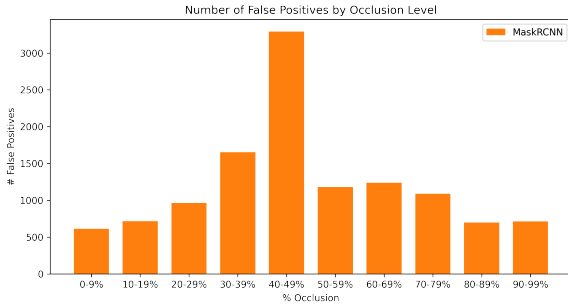
The detection of partially occluded pedestrians remains a persistent challenge for driver assistance systems and autonomous vehicles. Current methods of characterizing detection performance for partially occluded pedestrians have been broad, subjective, and inconsistent in their definition of the severity of occlusion. This research presents a novel test benchmark for the detailed, objective analysis of pedestrian detection models for partially occluded pedestrians. Detection performance is characterized for seven popular pedestrian detection models across a range of occlusion levels from 0-99%. Results demonstrate that detection performance experiences a linear decline as the occlusion level increases and the visibility of a pedestrian is reduced. An in-



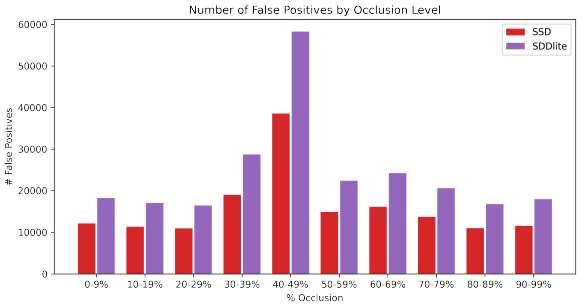
(a)



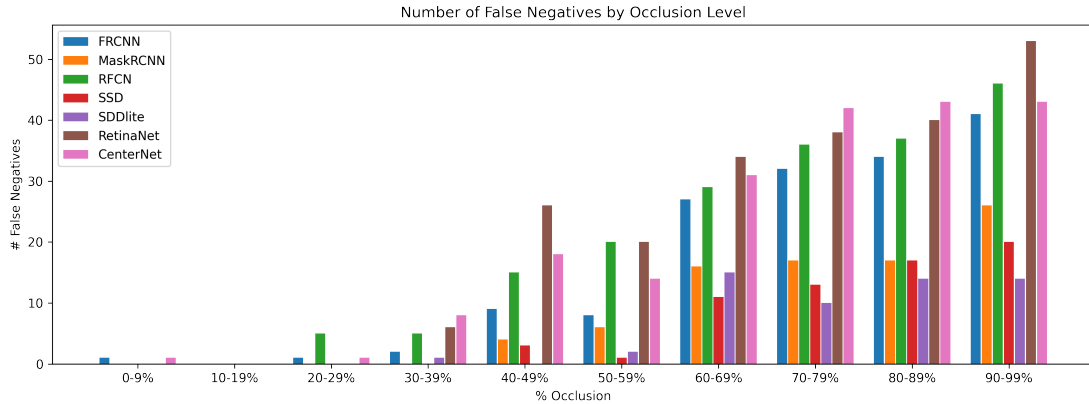
(b)



(c)



(d)



(e)

Figure 5. True Positives, False Positives and False Negatives. (a) displays the percentage of true positive detections by occlusion level for seven popular pedestrian detection models. (b), (c) and (d) display the number of false positives per occlusion level for each model. Note the differences in the Y-axis for each graph. (c) displays the number of false negatives by occlusion level. Results demonstrate that the number of false negative detections increase as the pedestrian occlusion level increases, and the percentage of true positive detections reduce significantly for pedestrians over 50% occluded.

crease in the number of false negative detections is observed as occlusion level increases and the percentage of true positive detections significantly degrade for pedestrians who are more than 50% occluded. Further analysis demonstrates that not all pedestrian detection models should be treated equally within an object detection system. The speed vs. accuracy trade-off, encouraged by the near real-time requirements of autonomous vehicles, can result in high lev-

els of false positive detections and lower detection confidence at progressive levels of pedestrian occlusion, particularly when using single stage detection models. Thorough objective characterization of pedestrian detection models at the design stage will improve the performance of object detection systems by calibrating the priority of detections in scenarios where known weaknesses can occur. System improvements may be gained through the use of an occlusion-

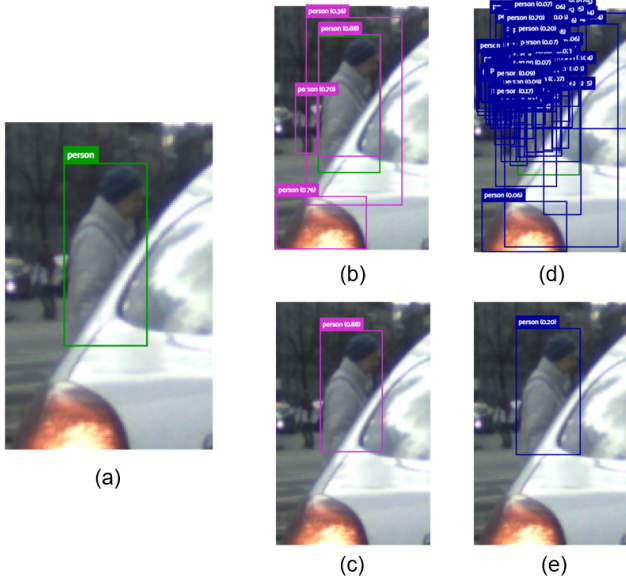


Figure 6. FasterRCNN vs. SSD. Detection performance is compared for a two stage network, FasterRCNN vs. a one stage network, SSD for an occluded pedestrian. The ground truth is shown in (a). FasterRCNN generates 4 proposals (b), 1 true positive detection with 88% confidence (c), and 3 false positives. SSD generates 84 detections (d), 1 true positive with 22% confidence (e), and 83 false positives.

aware step in the object detection pipeline to inform the priority of camera-based detections in sensor fusion networks for SAE level 4 and level 5 autonomous vehicles. In this manner, any reduction in performance at high occlusion levels can be mitigated in the design of the overall system to increase the safety of vulnerable road users and improve the efficiency of path planning based on environment detection. Widespread use of the proposed benchmark will result in more objective, consistent and detailed analysis of pedestrian detection models for partially occluded pedestrians.

References

- [1] S. international, "Taxonomy and definitions for terms related to driving automation systems for on-road motor vehicles," SAE, 2018. 1
- [2] S. Gilroy, E. Jones, and M. Glavin, "Overcoming occlusion in the automotive environment-a review," *IEEE Transactions on Intelligent Transportation Systems*, 2019. 1, 2
- [3] C. Ning, L. Menglu, Y. Hao, S. Xueping, and L. Yunhong, "Survey of pedestrian detection with occlusion," *Complex & Intelligent Systems*, vol. 7, no. 1, pp. 577–587, 2021. 1, 2
- [4] J. Cao, Y. Pang, J. Xie, F. S. Khan, and L. Shao, "From hand-crafted to deep features for pedestrian detection: A survey," *IEEE Transactions on Pattern Analysis and Machine Intelligence*, 2021. 1

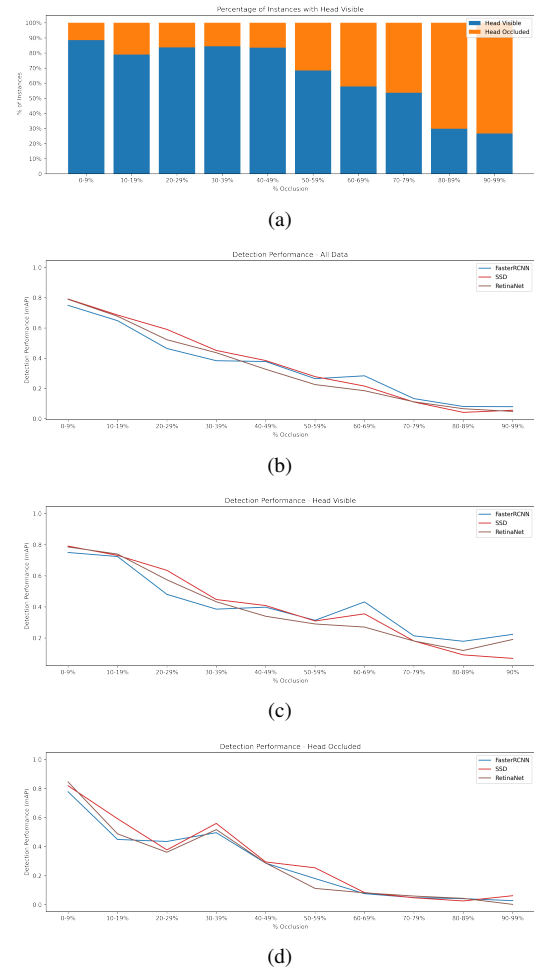


Figure 7. Analysis of data based on head visibility. (a) Dataset statistics based on head visibility. 820 total instances, 568 instances with head visible, 252 instances with head occluded. (b) Detection performance for FasterRCNN, SSD and RetinaNet for all data. (c) Detection performance for only images with head visible. Note, no occlusion level of more than 90% possible with head visible. (d) Detection performance for only images with head occluded. This analysis demonstrates that, in general, detection performance degrades as occlusion level increases regardless of the presence of key semantic features such as a pedestrian's head.

- [5] Y. Xiao, K. Zhou, G. Cui, L. Jia, Z. Fang, X. Yang, and Q. Xia, "Deep learning for occluded and multi-scale pedestrian detection: A review," *IET Image Processing*, 2021. 1, 2
- [6] S. Gilroy, M. Glavin, E. Jones, and D. Mullins, "Pedestrian occlusion level classification using keypoint detection and 2d body surface area estimation," in *Proceedings of the IEEE/CVF International Conference on Computer Vision*, pp. 3833–3839, 2021. 1, 2
- [7] A. Geiger, P. Lenz, and R. Urtasun, "Are we ready for autonomous driving? the kitti vision benchmark suite," in *2012*

- IEEE Conference on Computer Vision and Pattern Recognition*, pp. 3354–3361, IEEE, 2012. 1, 2
- [8] S. Zhang, R. Benenson, and B. Schiele, “Citypersons: A diverse dataset for pedestrian detection,” in *Proceedings of the IEEE Conference on Computer Vision and Pattern Recognition*, pp. 3213–3221, 2017. 1, 2
- [9] M. Braun, S. Krebs, F. Flohr, and D. M. Gavrila, “Eurocity persons: A novel benchmark for person detection in traffic scenes,” *IEEE transactions on pattern analysis and machine intelligence*, vol. 41, no. 8, pp. 1844–1861, 2019. 1, 2
- [10] S. Ren, K. He, R. Girshick, and J. Sun, “Faster r-cnn: towards real-time object detection with region proposal networks,” *IEEE transactions on pattern analysis and machine intelligence*, vol. 39, no. 6, pp. 1137–1149, 2016. 3, 5
- [11] B. E. Moore and J. J. Corso, “Fiftyone model zoo,” *Online*. https://voxel51.com/docs/fiftyone/user_guide/model_zoo, 2022. 3
- [12] K. He, G. Gkioxari, P. Dollár, and R. Girshick, “Mask r-cnn,” in *Proceedings of the IEEE international conference on computer vision*, pp. 2961–2969, 2017. 3, 5
- [13] J. Dai, Y. Li, K. He, and J. Sun, “R-fcn: Object detection via region-based fully convolutional networks,” in *Advances in neural information processing systems*, pp. 379–387, 2016. 3, 5
- [14] W. Liu, D. Anguelov, D. Erhan, C. Szegedy, S. Reed, C.-Y. Fu, and A. C. Berg, “Ssd: Single shot multibox detector,” in *European conference on computer vision*, pp. 21–37, Springer, 2016. 3, 4, 5
- [15] Pytorch, “Torchvision model zoo,” *Online*. <https://pytorch.org/vision/stable/models.html>, 2022. 3
- [16] A. Howard, M. Sandler, G. Chu, L.-C. Chen, B. Chen, M. Tan, W. Wang, Y. Zhu, R. Pang, V. Vasudevan, et al., “Searching for mobilenetv3,” in *Proceedings of the IEEE/CVF International Conference on Computer Vision*, pp. 1314–1324, 2019. 3, 4, 5
- [17] M. Sandler, A. Howard, M. Zhu, A. Zhmoginov, and L.-C. Chen, “Mobilenetv2: Inverted residuals and linear bottlenecks,” in *Proceedings of the IEEE conference on computer vision and pattern recognition*, pp. 4510–4520, 2018. 3, 4, 5
- [18] T.-Y. Lin, P. Goyal, R. Girshick, K. He, and P. Dollár, “Focal loss for dense object detection,” in *Proceedings of the IEEE international conference on computer vision*, pp. 2980–2988, 2017. 3, 4, 5
- [19] X. Zhou, D. Wang, and P. Krähenbühl, “Objects as points,” *arXiv preprint arXiv:1904.07850*, 2019. 3, 4, 5
- [20] P. Dollar, C. Wojek, B. Schiele, and P. Perona, “Pedestrian detection: An evaluation of the state of the art,” *IEEE transactions on pattern analysis and machine intelligence*, vol. 34, no. 4, pp. 743–761, 2011. 2
- [21] P. Dollár, C. Wojek, B. Schiele, and P. Perona, “Pedestrian detection: A benchmark,” in *2009 IEEE Conference on Computer Vision and Pattern Recognition*, pp. 304–311, IEEE, 2009. 2
- [22] S. Zhang, R. Benenson, M. Omran, J. Hosang, and B. Schiele, “How far are we from solving pedestrian detection?,” in *Proceedings of the IEEE conference on computer vision and pattern recognition*, pp. 1259–1267, 2016. 2
- [23] Y. Pang, J. Cao, Y. Li, J. Xie, H. Sun, and J. Gong, “Tjdhhd: A diverse high-resolution dataset for object detection,” *IEEE Transactions on Image Processing*, vol. 30, pp. 207–219, 2020. 2
- [24] S. Shao, Z. Zhao, B. Li, T. Xiao, G. Yu, X. Zhang, and J. Sun, “Crowdhuman: A benchmark for detecting human in a crowd,” *arXiv preprint arXiv:1805.00123*, 2018. 2
- [25] C. Chi, S. Zhang, J. Xing, Z. Lei, S. Z. Li, and X. Zou, “Pedhunter: Occlusion robust pedestrian detector in crowded scenes,” in *Proceedings of the AAAI Conference on Artificial Intelligence*, vol. 34, pp. 10639–10646, 2020. 2
- [26] X. Li, L. Li, F. Flohr, J. Wang, H. Xiong, M. Bernhard, S. Pan, D. M. Gavrila, and K. Li, “A unified framework for concurrent pedestrian and cyclist detection,” *IEEE transactions on intelligent transportation systems*, vol. 18, no. 2, pp. 269–281, 2016. 2
- [27] S. Hwang, J. Park, N. Kim, Y. Choi, and I. So Kweon, “Multispectral pedestrian detection: Benchmark dataset and baseline,” in *Proceedings of the IEEE conference on computer vision and pattern recognition*, pp. 1037–1045, 2015. 2
- [28] S. Walk, N. Majer, K. Schindler, and B. Schiele, “New features and insights for pedestrian detection,” in *2010 IEEE Computer society conference on computer vision and pattern recognition*, pp. 1030–1037, IEEE, 2010. 2
- [29] R. N. Rajaram, E. Ohn-Bar, and M. M. Trivedi, “An exploration of why and when pedestrian detection fails,” in *2015 IEEE 18th International Conference on Intelligent Transportation Systems*, pp. 2335–2340, IEEE, 2015. 2
- [30] J. Mao, T. Xiao, Y. Jiang, and Z. Cao, “What can help pedestrian detection?,” in *Proceedings of the IEEE Conference on Computer Vision and Pattern Recognition*, pp. 3127–3136, 2017. 2
- [31] S. Zhang, R. Benenson, M. Omran, J. Hosang, and B. Schiele, “Towards reaching human performance in pedestrian detection,” *IEEE transactions on pattern analysis and machine intelligence*, vol. 40, no. 4, pp. 973–986, 2017. 2
- [32] N. Ragesh and R. Rajesh, “Pedestrian detection in automotive safety: understanding state-of-the-art,” *IEEE Access*, vol. 7, pp. 47864–47890, 2019. 2
- [33] J. Cao, Y. Pang, J. Han, B. Gao, and X. Li, “Taking a look at small-scale pedestrians and occluded pedestrians,” *IEEE transactions on image processing*, vol. 29, pp. 3143–3152, 2019. 2
- [34] T. Toprak, B. A. Can, M. Ozcelikors, S. B. Tekin, and M. A. Selver, “Limitations of feature-classifier strategies on pedestrian detection for self driving cars,” in *2020 International Conference on Electrical, Communication, and Computer Engineering (ICECCE)*, pp. 1–6, IEEE, 2020. 2
- [35] I. Hasan, S. Liao, J. Li, S. U. Akram, and L. Shao, “Generalizable pedestrian detection: The elephant in the room,”

- in *Proceedings of the IEEE/CVF Conference on Computer Vision and Pattern Recognition*, pp. 11328–11337, 2021. 2
- [36] H. Chandel and S. Vatta, “Occlusion detection and handling: a review,” *International Journal of Computer Applications*, vol. 120, no. 10, 2015. 2
- [37] K. Saleh, S. Szénási, and Z. Vámosy, “Occlusion handling in generic object detection: A review,” in *2021 IEEE 19th World Symposium on Applied Machine Intelligence and Informatics (SAMI)*, pp. 000477–000484, IEEE, 2021. 2
- [38] S. Gilroy, M. Glavin, E. Jones, and D. Mullins, “An objective method for pedestrian occlusion level classification,” *arXiv preprint arXiv:2205.05412*, 2022. 2
- [39] A. Wallace, “The exposure treatment of burns,” *The Lancet*, vol. 257, no. 6653, pp. 501–504, 1951. 2
- [40] W.-S. Zheng, X. Li, T. Xiang, S. Liao, J. Lai, and S. Gong, “Partial person re-identification,” in *Proceedings of the IEEE International Conference on Computer Vision*, pp. 4678–4686, 2015. 2
- [41] J. Zhuo, Z. Chen, J. Lai, and G. Wang, “Occluded person re-identification,” in *2018 IEEE International Conference on Multimedia and Expo (ICME)*, pp. 1–6, IEEE, 2018. 2
- [42] T.-Y. Lin, M. Maire, S. Belongie, J. Hays, P. Perona, D. Ramanan, P. Dollár, and C. L. Zitnick, “Microsoft coco: Common objects in context,” in *European conference on computer vision*, pp. 740–755, Springer, 2014. 3
- [43] L. Chen, S. Lin, X. Lu, D. Cao, H. Wu, C. Guo, C. Liu, and F.-Y. Wang, “Deep neural network based vehicle and pedestrian detection for autonomous driving: A survey,” *IEEE Transactions on Intelligent Transportation Systems*, 2021. 3
- [44] B. E. Moore and J. J. Corso, “Fiftyone,” *GitHub*. Note: <https://github.com/voxel51/fiftyone>, 2020. 4